Convergence of stabilized $P1$ finite element scheme for time harmonic Maxwell's equations

M. Asadzadeh, L. Beilina

Abstract The paper considers the convergence study of the stabilized P1 finite element method for the time harmonic Maxwell's equations. The model problem is for the particular case of the dielectric permittivity function which is assumed to be constant in a boundary neighborhood. For the stabilized model a coercivity relation is derived that guarantee's the existence of a unique solution for the discrete problem. The convergence is addressed both in *a priori* and *a posteriori* settings. Our numerical examples validate obtained convergence results.

Key words: *time harmonic Maxwell's equations*, P_1 *finite elements*, *a priori estimate*, *a posteriori estimate*, *convergence*

1 Introduction

In implementing the finite element methods for the Maxwell system, the divergence-free edge elements are the most advantageous from a theoretical point of view [12, 13]. On the other hand for the time-dependent problems, where a linear system of equations need to be solved at each iteration step, the divergence-free approach requires an unrealistic fine degree of time resolution. To circumvent this difficulty, it has been suggested to use the continuous P1 finite elements which provides inexpensive and reliable algorithms for the numerical simulations, in particular compared to $H(curl)$ conforming finite elements. Based on this fact, in this paper we consider stabilized P1 finite element for the approximate solution of time

L. Beilina
Department of Mathematical Sciences, Chalmers University of Technology and University of Gothenburg , SE-412 96 Gothenburg Sweden, e-mail: larisa.beilina@chalmers.se

M. Asadzadeh
Department of Mathematical Sciences, Chalmers University of Technology and University of Gothenburg , SE-412 96 Gothenburg Sweden, e-mail: mohammad@chalmers.se

harmonic Maxwell's equations when the dielectric permittivity function is constant in a boundary neighborhood. This converts the Maxwell's equations into a set of time-independent wave equations on the boundary neighborhood.

An outline of this paper is as follows. In Section 2 we introduce a model problem for the time harmonic Maxwell's equations obtained through Laplace transform of the time-dependent equations. In Section 3 we introduce our finite element scheme, prove its well-posedness. as well as a optimal a priori and a posteriori error bounds which are derived in a, gradient dependent, triple norm. In the a posteriori case the boundary residual is in the form of a normal derivative and therefore is balanced by a multiplicative power of the mesh parameter h. Section 4 is devoted to implementations and justify the robustness of the approximation procedure. Finally, in Section 5 we conclude the results of the paper.

Throughout the paper C will denote a generic constant, not necessarily the same at each occurrence and independent of the mesh parameter and solution, unless otherwise specifically specified.

2 The mathematical model

We study the time-harmonic Maxwell's equations for electric field $\hat{E}(x,s)$, under the assumption of the vanishing electric charges, given by

$$\begin{gathered} s^2\varepsilon(x)\hat{E}(x,s) + \nabla\times\nabla\times\hat{E}(x,s) = s\varepsilon(x) f_0(x), \;\; x\in\mathbb{R}^d, \quad d=2,3 \\ \nabla\cdot(\varepsilon(x)\hat{E}(x,s)) = 0 \end{gathered} \tag{1}$$

where $\varepsilon(x) = \varepsilon_r(x)\varepsilon_0$ is the dielectric permittivity, $\varepsilon_r(x)$ is the dimensionless relative dielectric permittivity and ε_0 is the permittivity of the free space. Furthermore

$$\nabla\times\nabla\times E = \nabla(\nabla\cdot E) - \nabla^2 E. \tag{2}$$

The equation (1) is obtained through the Laplace transformation in time

$$\widehat{E}(x,s) := \int_0^{+\infty} E(x,t)e^{-st}\,dt, \qquad s = const. > 0 \tag{3}$$

where $E(x,t)$ is the the solution of time-dependent Maxwell's equations:

$$\begin{gathered} \varepsilon(x)\frac{\partial^2 E(x,t)}{\partial t^2} + \nabla\times\nabla\times E(x,t) = 0, \;\; x\in\mathbb{R}^d, d=2,3, \; t\in(0,T]. \\ \nabla\cdot(\varepsilon E)(x,t) = 0, \\ E(x,0) = f_0(x), \quad \frac{\partial E}{\partial t}(x,0) = 0, \;\; x\in\mathbb{R}^d, \quad d=2,3. \end{gathered} \tag{4}$$

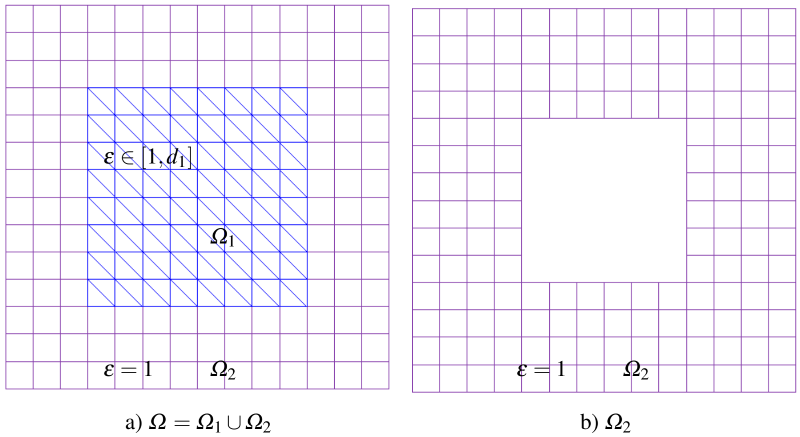

Fig. 1 *Domain decomposition in* Ω.

Note that, since we have a non-zero initial condition: $E(x,0) = f_0(x)$, the problem (4) is adequate as a coefficient inverse problem to determine the function $\varepsilon(x)$ in (4) through a finite number of observations E at the boundary [6].

To solve the problem (4) numerically, we consider it in a bounded convex and simply connected polygonal domain $\Omega \subset \mathbb{R}^d, d = 2,3$ with boundary Γ: We define $\Omega_2 := \Omega \setminus \Omega_1$, where $\Omega_1 \subset \Omega$ has positive Lebesgue measure and $\partial\Omega \cap \partial\Omega_1 = \emptyset$. In this setting cutting out Ω_1 from Ω, the new subdomain Ω_2 shares the boundary with both Ω and Ω_1: $\partial\Omega_2 = \partial\Omega \cup \partial\Omega_1$, $\Omega = \Omega_1 \cup \Omega_2$, $\Omega_1 = \Omega \setminus \Omega_2$ and $\bar{\Omega}_1 \cap \bar{\Omega}_2 = \partial\Omega_1$, (see Fig. 1).

To proceed we assume that $\varepsilon(x) \in C^2(\mathbb{R}^d), d = 2,3$ satisfies

$$\begin{aligned} \varepsilon(x) &\in [1, d_1], && \text{for } x \in \Omega_1, \\ \varepsilon(x) &= 1, && \text{for } x \in \Omega \setminus \Omega_1, \\ \partial_\nu \varepsilon &= 0, && \text{for } x \in \partial\Omega_2. \end{aligned} \tag{5}$$

Remark 1. Conditions (5) mean that, in the vicinity of the boundary of the computational domain Ω, the equation (4) transforms to a time-dependent wave equation.

At the boundary $\Gamma := \partial\Omega$ of Ω, we use the split $\Gamma = \Gamma_1 \cup \Gamma_2 \cup \Gamma_3$, so that Γ_1 and Γ_2 are the top and bottom sides, with respect to y- (in $2d$) or z-axis (in $3d$), of the domain Ω, respectively, while Γ_3 is the rest of the boundary. Further, $\partial_\nu(\cdot)$ denotes the normal derivative on Γ and ν is the outward unit normal to Γ.

Remark 2. In most estimates below, it suffices to restrict the Neumann boundary condition for the dielectric permittivity function to: $\partial_\nu \varepsilon(x) = 0$, on $\Gamma_1 \cup \Gamma_2$.

Now, using similar argument as in the studies in, e.g., [5] and by Remark 1, for the time-dependent wave equation, we impose first order absorbing boundary condition [11] at $\Gamma_1 \cup \Gamma_2$:

$$\partial_\nu E + \partial_t E = 0, \qquad (x,t) \in (\Gamma_1 \cup \Gamma_2) \times (0,T]. \tag{6}$$

To impose boundary conditions at Γ_3 we can assume that the surface Γ_3 is located far from the domain Ω_1. Hence, we can assume that $E \approx E^{inc}$ in a vicinity of Γ_3, where E^{inc} is the incident field. Thus, at Γ_3 we may impose Neumann boundary condition

$$\partial_\nu E = 0, \qquad (x,t) \in \Gamma_3 \times (0,T]. \tag{7}$$

Finally, using the well known vector-analysis relation (2) and applying the Laplace transform to the equation (4) and the boundary conditions (6)-(7) in the time domain, the problem (1) will be transformed to the following model problem

$$\begin{aligned} s^2\varepsilon(x)\hat{E}(x,s) + \nabla(\nabla\cdot\hat{E}(x,s)) - \triangle\hat{E}(x,s) &= s\varepsilon(x)f_0(x), \;\; x\in\mathbb{R}^d, d=2,3 \\ \nabla\cdot(\varepsilon(x)\hat{E}(x,s)) &= 0, \\ \partial_\nu\hat{E}(x,s) &= 0, \quad x\in\Gamma_3, \\ \partial_\nu\hat{E}(x,s) &= f_0(x) - s\hat{E}(x,s), \; x\in\Gamma_1\cup\Gamma_2. \end{aligned} \tag{8}$$

3 Finite element method

We have the usual notation of the inner product in $[L_2(\Omega)]^d$: $(\cdot,\cdot)$, $d\in\{2,3\}$, and the corresponding norm $\|\cdot\|$, whereas $\langle\cdot,\cdot\rangle_\Gamma$ is the inner product of $[L_2(\Gamma)]^{d-1}$ and the associated $L_2(\Gamma)$-norm is denoted by $\|\cdot\|_\Gamma$. We define the L_2 scalar products

$$(u,v) := \int_\Omega u\cdot v\,d\mathbf{x}, \quad (u,v)_\omega := \int_\Omega u\cdot v\;\omega d\mathbf{x}, \quad \langle u,v\rangle_\Gamma := \int_\Gamma u\cdot v\,d\sigma,$$

and the ω-weighted $L^2(\Omega)$ norm

$$\|u\|_\omega := \sqrt{\int_\Omega |u|^2\,\omega d\mathbf{x}}, \qquad \omega>0, \quad \omega\in L^\infty(\Omega).$$

3.1 Stabilized model

The stabilized formulation of the problem (8), with $d=2,3$, reads as follows:

$$\begin{aligned} s^2\varepsilon(x)\hat{E}(x,s) - \triangle\hat{E}(x,s) - \nabla(\nabla\cdot((\varepsilon-1)\hat{E}(x,s)) &= s\varepsilon(x)f_0(x) \quad x\in\mathbb{R}^d, \\ \partial_\nu\hat{E}(x,s) &= 0, \quad x\in\Gamma_3, \\ \partial_\nu\hat{E}(x,s) &= f_0(x) - s\hat{E}(x,s), \quad x\in\Gamma_1\cup\Gamma_2, \end{aligned} \tag{9}$$

where the second equation of (8) is hidden in the first one.

3.2 Finite element discretization

We consider a partition of Ω into elements K denoted by $\mathscr{T}_h = \{K\}$, satisfying the minimal angle condition. Here, $h = h(x)$ is the mesh parameter defined as $h|_K = h_K$, representing the local diameter of the elements. We also denote by $\partial \mathscr{T}_h = \{\partial K\}$ a partition of the boundary Γ into boundaries ∂K of the elements K such that vertices of these elements lie on Γ.

To formulate the finite element method for (9) in Ω, we introduce the, piecewise linear, finite element space $W_h^E(\Omega)$ for every component of the electric field E:

$$W_h^E(\Omega) := \{w \in H^1(\Omega) : w|_K \in P_1(K),\ \forall K \in \mathscr{T}_h\},$$

where $P_1(K)$ denote the set of piecewise-linear functions on K. Setting $\mathbf{W}_h^E(\Omega) := [W_h^E(\Omega)]^3$ we define f_{0h} to be the $\mathbf{W}_h^E$-interpolant of f_0 in (9). Then the finite element method for the problem (9) is formulated as: *Find* $\hat{E}_h \in \mathbf{W}_h^E(\Omega)$ *such that* $\forall \mathbf{v} \in \mathbf{W}_h^E(\Omega)$

$$\begin{aligned} &(s^2 \varepsilon \hat{E}_h, \mathbf{v}) + (\nabla \hat{E}_h, \nabla \mathbf{v}) + (\nabla \cdot (\varepsilon \hat{E}_h), \nabla \cdot \mathbf{v}) - (\nabla \cdot \hat{E}_h, \nabla \cdot \mathbf{v}) \\ &+ \langle s\hat{E}_h, \mathbf{v} \rangle_{\Gamma_1 \cup \Gamma_2} = (s\varepsilon f_{0h}, \mathbf{v}) + \langle f_{0h}, \mathbf{v} \rangle_{\Gamma_1 \cup \Gamma_2}. \end{aligned} \tag{10}$$

Theorem 1 (well-posedness). *Under the condition*

$$f_{0,h} \in L_{2,\varepsilon} \cap L_{2,1/s}(\Gamma_1 \cup \Gamma_2), \tag{11}$$

on the data, the problem (10) *has a unique solution* $\hat{E}_h \in \boldsymbol{W}_h^E(\Omega)$.

Proof. See [1].

3.3 Error analysis

In this subsection first we give a swift a priori error bound and then continue with a posteriori error estimates. For the sake of completeness, we set up an adaptive algorithm for the a posteriori setting. This, however, requires a thorough and lengthy implementations procedure which is beyond the scope of the present paper and may be considered in a future study.

3.3.1 A priori error estimates

To derive a priori error estimates we consider the continuous variational formulation and define linear and bilinear forms in the finite element space $\mathbf{W}_h^E(\Omega)$:

$$
\begin{aligned}
a(\hat{E}, \mathbf{v}) = &(s^2 \varepsilon \hat{E}, \mathbf{v}) + (\nabla \hat{E}, \nabla \mathbf{v}) + (\nabla \cdot (\varepsilon \hat{E}), \nabla \cdot \mathbf{v}) \\
&- (\nabla \cdot \hat{E}, \nabla \cdot \mathbf{v}) + \langle s\hat{E}, \mathbf{v} \rangle_{\Gamma_1 \cup \Gamma_2}, \qquad \forall \mathbf{v} \in H^1(\Omega)
\end{aligned} \tag{12}
$$

and

$$
\mathscr{L}^c(\mathbf{v}) := (s\varepsilon f_0, \mathbf{v}) + \langle f_0, \mathbf{v} \rangle_{\Gamma_1 \cup \Gamma_2}, \qquad \forall \mathbf{v} \in H^1(\Omega). \tag{13}
$$

Hence we have the concise form of the variational formulation

$$
a(\hat{E}, \mathbf{v}) = \mathscr{L}^c(\mathbf{v}), \qquad \forall \mathbf{v} \in H^1(\Omega). \tag{14}
$$

This yields the *Galerkin orthogonality* [7] by letting, in (12) and (13), $\mathbf{v} \in \mathbf{W}_h^E(\Omega)$, as well as replacing f_0 by $f_{0,h}$ in (13). Subtracting from (14) its discrete version and letting $e(x,s) := \hat{E}(x,s) - \hat{E}_h(x,s)$ be the pointwise spatial error of the finite element approximation (10), we get

$$
a(\hat{E} - \hat{E}_h, \mathbf{v}) = 0, \qquad \forall \mathbf{v} \in \mathbf{W}_h^E(\Omega), \qquad \text{(Galerkin orthogonality)}. \tag{15}
$$

Now we are ready to derive the following theoretical error bound

Theorem 2. *Let $\hat{E}$ and $\hat{E}_h$ be the solutions for the continuous problem* (9) *and its finite element approximation,* (10)*, respectively. Then, there is a constant C, independent of $\hat{E}$ and h, such that*

$$
|||e||| \leq C \parallel h\hat{E} \parallel_{H_w^2(\Omega)} .
$$

where $w = w(\varepsilon(x), s)$ is the weight function which depends on the dielectric permittivity function $\varepsilon(x)$ and the pseudo-frequency variable s.

Proof. See the proof of Theorem 2 in [1].

3.3.2 A posteriori error estimates

For the approximate solution $\hat{E}_h = \hat{E}_h(x,s)$ of the problem (9), we define the residual errors

$$
\begin{aligned}
-\mathscr{R}(\hat{E}_h) := &s^2 \varepsilon(x) \hat{E}_h - \triangle \hat{E}_h - \nabla(\nabla \cdot ((\varepsilon(x) - 1)\hat{E}_h) - s\varepsilon(x) f_{0,h}(x), \quad \text{and} \\
-\mathscr{R}_\Gamma(\hat{E}_h) := &h^{-\alpha} \Big(\partial_\nu \hat{E}_h + s\hat{E}_h - f_{0,h}(x) \Big), \quad \text{for} \quad x \in \Gamma_1 \cup \Gamma_2, \quad 0 < \alpha \leq 1.
\end{aligned} \tag{16}
$$

By the Galerkin orthogonality we have that $\mathscr{R}(\hat{E}_h) \perp \mathbf{W}_h^E(\Omega)$. Now the objective is to bound the triple norm of the error $e(x,s) := \hat{E}(x,s) - \hat{E}_h(x,s)$ by some adequate norms of $\mathscr{R}(\hat{E}_h)$ and $\mathscr{R}_\Gamma(\hat{E}_h)$ with a relevant, fast, decay. This may be done in a few, relatively similar, ways, e.g., one can use the variational formulation and interpolation in the error combined with Galerkin orthogonality. Or one may use a dual problem approach setting the source term (or initial data) on the right hand side as the error.

The proof of the main result relies on assuming a first order approximation for the initial value of the original field $f_0(x) := E(x,t)|_{t=0_-}$, for $\beta \approx 1$, viz,

$$\| f_0 - f_{0,h} \|_\varepsilon \approx \| f_0 - f_{0,h} \|_{1/s,\Gamma} \approx \| f_0 - f_{0,h} \|_{(\varepsilon-1)^2/s,\Gamma} = \mathscr{O}(h^\beta). \tag{17}$$

Theorem 3. *Let $\hat{E}$ and $\hat{E}_h$ be the solutions for the continuous problem* (9) *and its finite element approximation* (10)*, respectively. Further we assume that we have the error bound* (17) *for the initial field $f_0(x) := E(x,t)|_{t=0_-}$. Then, there exist interpolation constants C_1 and C_2, independent of h, and $\hat{E}$, but may depend on ε and s such that the following a posteriori error estimate holds true*

$$|||e||| \le C_1\, h \,\| \mathscr{R} \| + C_2\, h^\alpha \,\| \mathscr{R}_\Gamma \|_{1/s,\Gamma_1\cup\Gamma_2} + \mathscr{O}(h^\beta), \tag{18}$$

where $\alpha \approx \beta \approx 1$.

Proof. See [1]

An adaptivity algorithm

Given an *admissible* small error tolerance $TOL > 0$, we outline formal adaptivity steps to reach

$$|||e||| \le TOL. \tag{19}$$

To this end we start with a course mesh with mesh size h and

Step 1. Compute the approximate solution $\hat{E}_h$ and its corresponding domain and boundary residuals $\mathscr{R}$ and $\mathscr{R}_\Gamma$, respectively.

Step 2. Check whether

$$C_1\, h \,\| \mathscr{R} \| + C_2\, h^\alpha \,\| \mathscr{R}_\Gamma \|_{1/s,\Gamma_1\cup\Gamma_2} + \mathscr{O}(h^\beta) \le TOL? \tag{20}$$

for $\alpha \approx \beta \approx 1$.

Step 3. If (20) is valid stop and accept the current h-function. Otherwise, refine in regions where the contribution to the right hand side in (18) is *large* (on each iteration step you need to choose a criterion for this *largeness*). Replace the h-function by the new refined one and go to Step 1.

4 Numerical examples

We refer to [1] for complete description of numerical tests. Numerical tests are performed in the computational domain $\Omega = [0,1] \times [0,1]$. The source data $f(x), x \in$

$\mathbb{R}^2$ (the right hand side) in the model problem (8) for the electric field $\hat{E} = (\hat{E}_1, \hat{E}_2)$ is chosen such that the function

$$\begin{aligned} \hat{E}_1 &= \frac{2}{s^3 \varepsilon} \pi \sin^2 \pi x \cos \pi y \sin \pi y, \\ \hat{E}_2 &= -\frac{2}{s^3 \varepsilon} \pi \sin^2 \pi y \cos \pi x \sin \pi x. \end{aligned} \tag{21}$$

is the exact solution of the model problem (8).

We define the function ε as

$$\varepsilon(x,y) = \begin{cases} 1 + \sin^m \pi(2x - 0.5) \cdot \sin^m \pi(2y - 0.5) & \text{in } [0.25, 0.75] \times [0.25, 0.75], \\ 1 & \text{otherwise.} \end{cases} \tag{22}$$

for an integer $m > 1$.

The computational domain Ω is discretized into triangles K of sizes $h_l = 2^{-l}, l = 1, ..., 6$. Numerical tests are performed for different $m = 2, ..., 9$ in (22), $s = 20$ in (8), and the relative errors e_l^1, e_l^2 are measured in L_2-norm and the H^1-norms, respectively, which we compute as

$$e_l^1 = \frac{\|\hat{E} - \hat{E}_h\|_{L_2}}{\|\hat{E}\|_{L_2}}, \tag{23}$$

$$e_l^2 = \frac{\|\nabla(\hat{E} - \hat{E}_h)\|_{L_2}}{\|\nabla \hat{E}\|_{L_2}}. \tag{24}$$

Here,

$$\hat{E} := \sqrt{\hat{E}_1^2 + \hat{E}_2^2} \qquad \hat{E}_h := \sqrt{\hat{E}_{1h}^2 + \hat{E}_{2h}^2}. \tag{25}$$

Figure 2 presents convergence of P1 finite element scheme for $m = 2, 9$ in (22). Tables 1-2 present convergence rates q_1, q_2 for $m = 2, 9$ which we compute as

$$q_1 = \frac{\log\left(\frac{e^1_{l\,h}}{e^2_{l\,2h}}\right)}{\log(0.5)}, \quad q_2 = \frac{\log\left(\frac{e^2_{l\,h}}{e^2_{l\,2h}}\right)}{\log(0.5)}, \tag{26}$$

where $e^i_{lh}, e^i_{l2h}, i = 1,2,$ are computed relative norms $e^i_l, i = 1,2,$ on the finite element mesh with the mesh size h and $2h$, respectively. Similar convergence rates are obtained for $m = 3,4,5,8$. Figure (3) shows computed and exact solutions on different finite element meshes for $m = 2$ and $m = 9$ in (22). We observe that our P1 finite element scheme behaves like a first order method for $H^1(\Omega)$-norm and second order method for $L^2(\Omega)$-norm.

l	nel	nno	e_l^1	q_1	e_l^2	q_2
1	8	9	$2.71 \cdot 10^{-2}$		$8.60 \cdot 10^{-2}$	
2	32	25	$6.66 \cdot 10^{-3}$	2.02	$3.25 \cdot 10^{-2}$	1.40
3	128	81	$1.78 \cdot 10^{-3}$	1.90	$1.75 \cdot 10^{-2}$	$8.99 \cdot 10^{-1}$
4	512	289	$4.13 \cdot 10^{-4}$	2.11	$1.02 \cdot 10^{-2}$	$7.79 \cdot 10^{-1}$
5	2048	1089	$1.05 \cdot 10^{-4}$	1.97	$5.29 \cdot 10^{-3}$	$9.42 \cdot 10^{-1}$
6	8192	4225	$2.65 \cdot 10^{-5}$	1.99	$2.70 \cdot 10^{-3}$	$9.69 \cdot 10^{-1}$

Table 1 Relative errors in the L_2-norm and in the H^1-norm for mesh sizes $h_l = 2^{-l}, l = 1, ..., 6$, for $m = 2$ in (22). Here, *nel* is number of elements and *nno* is number of nodes in the mesh.

l	nel	nno	e_l^1	q_1	e_l^2	q_2
1	8	9	$1.73 \cdot 10^{-2}$		$7.29 \cdot 10^{-2}$	
2	32	25	$3.33 \cdot 10^{-3}$	2.38	$3.57 \cdot 10^{-2}$	1.03
3	128	81	$8.98 \cdot 10^{-4}$	1.89	$2.15 \cdot 10^{-2}$	$7.33 \cdot 10^{-1}$
4	512	289	$2.36 \cdot 10^{-4}$	1.93	$1.08 \cdot 10^{-2}$	$9.94 \cdot 10^{-1}$
5	2048	1089	$6.09 \cdot 10^{-5}$	1.96	$5.26 \cdot 10^{-3}$	1.04
6	8192	4225	$1.55 \cdot 10^{-5}$	1.98	$2.62 \cdot 10^{-3}$	1.00

Table 2 Relative errors in the L_2-norm and in the H^1-norm for mesh sizes $h_l = 2^{-l}, l = 1, ..., 6$, for $m = 9$ in (22). Here, *nel* is number of elements and *nno* is number of nodes in the mesh.

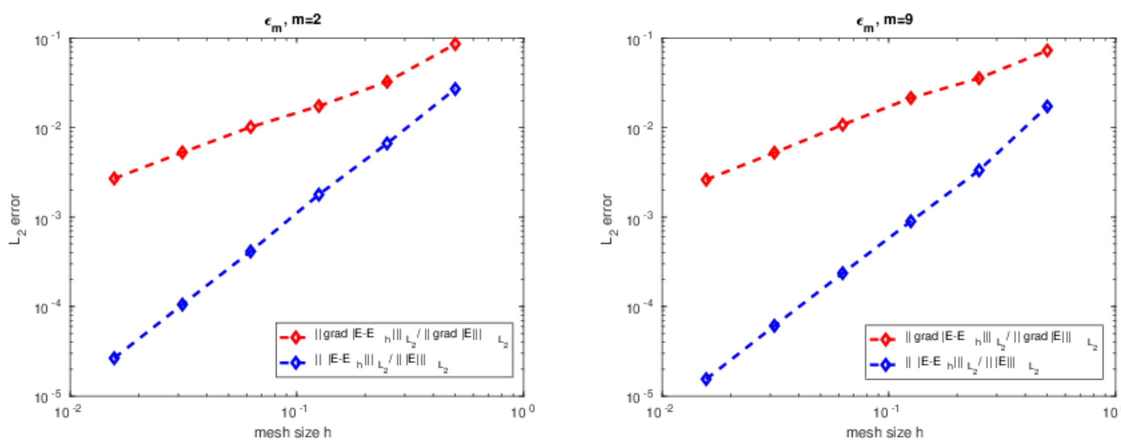

Fig. 2 Relative errors for $m = 2$ (left) and $m = 9$ (right).

5 Conclusion

We presented convergence analysis for the stabilized P1 finite element scheme applied to the solution of time harmonic Maxwell's equations with constant dielectric permittivity function $\varepsilon(x)$ in a boundary neighborhood. For the convergence study of stabilized P1 finite element method for a time dependent problem for Maxwell's equations we refer to [2]. Optimal a priori and a posteriori error bounds are derived

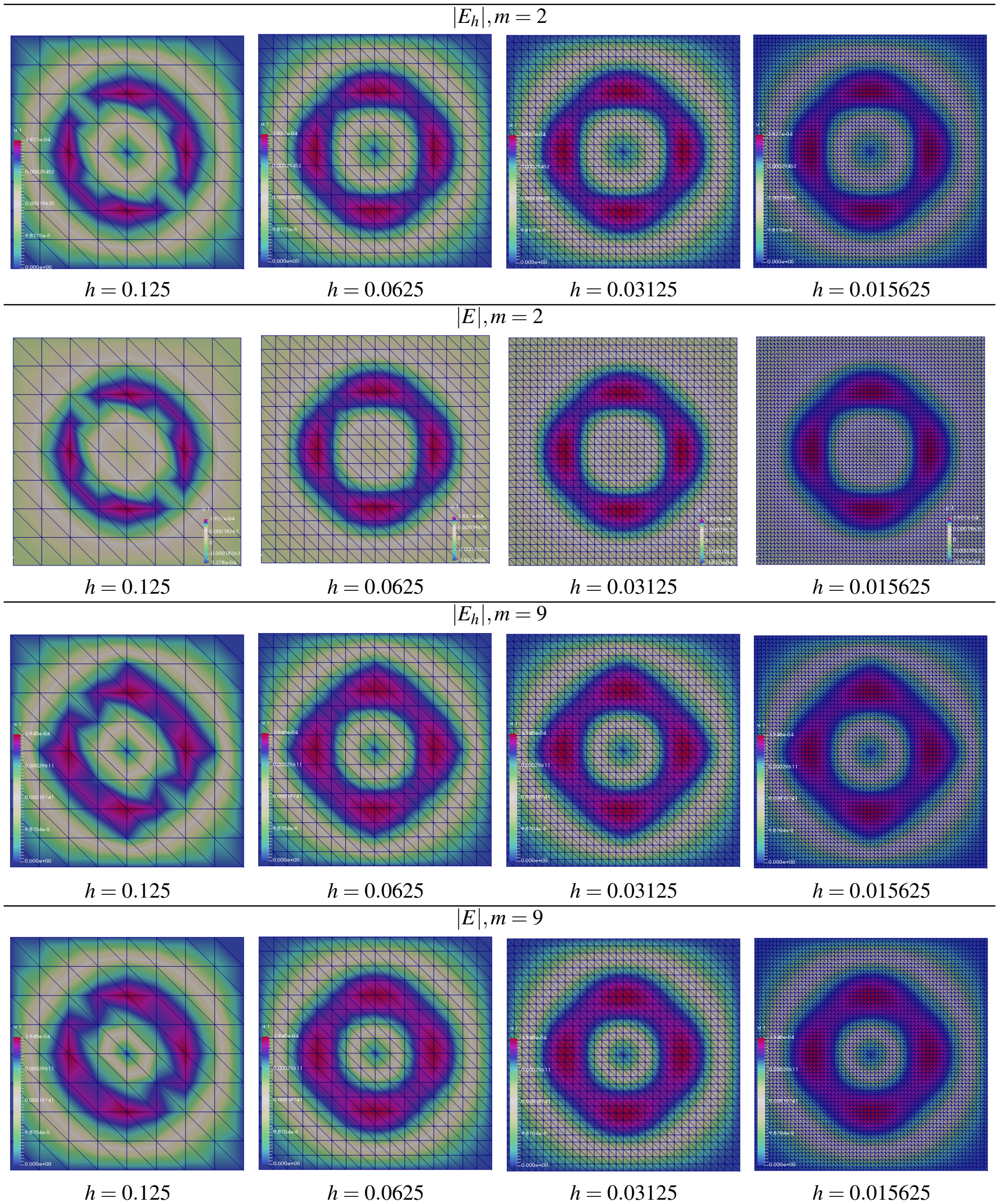

Fig. 3 *Computed vs. exact solution for different meshes taking* $m = 2$ *and* $m = 9$ *in* (22).

in weighted energy norms and numerical results validate obtained theoretical error bounds.

Proposed scheme can be applied for the solution of coefficient inverse problems with constant dielectric permittivity function in a boundary neighborhood, see [3, 4, 5, 8, 9, 10, 14, 15] for a such problems.

References

1. M. Asadzadeh, L. Beilina, On stabilized P1 finite element approximation fortime harmonic Maxwell's equations, https://arxiv.org/abs/1906.02089, 2019.
2. L. Beilina, V. Ruas, An explicit P1 finite element scheme for Maxwell's equations with constant permittivity in a boundary neighborhood, arXiv:1808.10720.
3. L. Beilina and M. V. Klibanov, *Approximate global convergence and adaptivity for Coefficient Inverse Problems*, Springer, New York, 2012.
4. L. Beilina, N. T. Th'anh, M. Klibanov, and J. B. Malmberg, Reconstruction of shapes and refractive indices from blind backscattering experimental data using the adaptivity, *Inverse Problems*, 30 (2014), 105007.
5. L. Beilina, N. T. Th'anh, M.V. Klibanov and J. B. Malmberg, Globally convergent and adaptive finite element methods in imaging of buried objects from experimental backscattering radar measurements, *Journal of Computational and Applied Mathematics, Elsevier*, DOI: 10.1016/j.cam.2014.11.055, 2015.
6. M. Bellassoued, M. Cristofol, and E. Soccorsi, Inverse boundary value problem for the dynamical heterogeneous Maxwell's system, *Inverse Problems*, 28, 095009(188pp), 2012.
7. S. C. Brenner and L. R. Scott, *The Mathematical Theory of Finite Element Methods*, Springer-Verlag, Berlin, 1994.
8. J. Bondestam Malmberg, L. Beilina, An Adaptive Finite Element Method in Quantitative Reconstruction of Small Inclusions from Limited Observations, *Appl. Math. Inf. Sci.*, 12(1), 1-19, 2018.
9. V. A. Burov, S. A. Morozov, and O. D. Rumyantseva, Reconstruction of fine-scale structure of acoustical scatterers on large-scale contrast background, *Acoustical Imaging*, 26 (2002), pp. 231-238.
10. A. E. Bulyshev, A. E. Souvorov, S. Y. Semenov, V. G. Posukh and Y. E. Sizov, Three-dimensional vector microwave tomography: theory and computational experiments, *Inverse Problems*, 20(4), pp.1239-1259, 2004.
11. B. Engquist and A. Majda, Absorbing boundary conditions for the numerical simulation of waves, *Math. Comp.*, 31, 629-651, 1977.
12. P. B. Monk, *Finite Element methods for Maxwell's equations*, Oxford University Press, 2003.
13. J.-C. Nédélec, Mixed finite elements in R3, *Numerische Mathematik*, 35 (1980), 315-341.
14. N. T. Thánh, L. Beilina, M. V. Klibanov, and M. A. Fiddy, Reconstruction of the refractive index from experimental backscattering data using a globally convergent inverse method, *SIAMJ. Sci. Comput.*, 36 (2014), pp. B273-B293.
15. N. T. Thánh, L. Beilina, M. V. Klibanov, M. A. Fiddy, Imaging of Buried Objects from Experimental Backscattering Time-Dependent Measurements using a Globally Convergent Inverse Algorithm, *SIAM Journal on Imaging Sciences*, 8(1), 757-786, 2015.